Science Advances
AAAS

Supplementary Materials for

Leukemic progenitor cells enable immunosuppression and post-chemotherapy relapse via IL-36–inflammatory monocyte axis

He-Zhou Guo, Zi-Hua Guo, Shan-He Yu, Li-Ting Niu, Wan-Ting Qiang, Meng-Meng Huang, Yuan-Yuan Tian, Juan Chen, Hui Yang, Xiang-Qin Weng, Yi Zhang, Wu Zhang, Shao-Yan Hu, Jun Shi*, Jiang Zhu*

*Corresponding author. Email: zhujiang@shsmu.edu.cn (J.Z.); junshi@sjtu.edu.cn (J.S.)

Published 8 October 2021, *Sci. Adv.* **7**, eabg4167 (2021)
DOI: 10.1126/sciadv.abg4167

This PDF file includes:

Supplementary Materials and Methods

Reagents

Cytarabine (Selleck Chemicals; S1648). Doxorubicin (Selleck Chemicals; S1208). Nor-NOHA (ApexBio Technology; C5407). SC75741 (MedChem Express; HY-10496). U0126 (MedChem Express; HY-12031A). Stattic (MedChem Express; HY-13818). L-NMMA (MedChem Express; HY-18732A). Trabectedin (MedChem Express; HY-50936). VX-765 (MedChem Express; HY-13205). Clodronate liposomes and Control liposomes (LIPOSOMA; CP-005-005). Recombinant human IL-36γ (R&D Systems; 6835-IL-010). Recombinant mouse IL-36γ (R&D Systems; 6996-IL-010). Recombinant human IL-36Ra (R&D Systems; 1275-IL-025). Recombinant mouse IL-36Ra (R&D Systems; 2714-ML-025). Recombinant human IL-36α (R&D Systems; 6995-IL-010). Doxycycline (Clontech; 631311). Anti-mouse IL-1β antibody (R&D Systems; AF-401-NA). Anti-mouse NK1.1 antibody (Bio X cell; BE0036). Anti-mouse CD8β antibody (Bio X cell; BE0223). Anti-mouse PD-1 antibody (Bio X cell; BP0146). Isotype control antibody (Bio X cell; BE0085, BE0088, BE0075, BP0089).

Conditional medium

To make conditional medium (CM), mouse leukemia cells (5×10^6 cells/ml) cultured with IMDM containing 10% FBS, 50 ng/ml mSCF, 10 ng/ml mIL-6, 6 ng/ml mIL-3 for 30 hours. Then, the supernatant was collected as CM. Human leukemia cells (5×10^6 cells/ml) were cultured with IMDM supplemented with 20% BIT for 30 hours. Then, the supernatant was collected as CM. In some experiments, Ara-C (80 nM) and VX-765 (100 μM) were added.

Cytokines array

The Bio-Plex Magpix System (BIO-RAD) was used to measure the levels of relevant cytokines in mouse bone marrow supernatant. Bio-Plex Pro Mouse Cytokine 23-Plex Panel (BIO-RAD;

M60009RDPD), Bio-Plex Pro Mouse Cytokine 9-Plex Panel (BIO-RAD; MD000000EL) and Bio-Plex Pro Mouse Cytokine Th17 Panel A 6-Plex Panel (BIO-RAD; M6000007NY) were used.

Il-36R knockdown hematopoietic chimeric mice

Il-36R shRNAs were cloned into lentiviral plasmid that express mCherry to produce lentivirus. Lineage$^-$ bone marrow cells derived from FVB/NJ mice were infected with this lentivirus. The transduced mCherry$^+$ cells were sorted out and transplanted into lethally irradiated (9 Gy) FVB/NJ mice to make chimeric mice. The shRNA target sequences are as follow: 5′-CCAGATGTGTACCAGCAAATA-3′.

Quantification of cytokines

Cytokine concentrations were measured using specific ELISA kits, including those for mouse Il-36γ (Cloud-Clone Corp; SEL621Mu), mouse Il-1β (R&D Systems; MLB00C), human IL-36α (R&D Systems; DY1078-05), human IL-1β (R&D Systems; DLB50) according to the manufacturers' instructions.

Quantitative real-time RT-PCR:

Total cellular RNA was extracted using the EZ-press RNA purification kit (EZBioscience; B0004plus) following the manufacturer's protocol. The cDNA was synthesized through reverse transcription of 1 μg of RNA using ReverTra Ace-αTM (TOYOBO; FSQ-101). Quantitative real-time RT-PCR reactions were performed using TB Green Premix Ex Taq (Takara; RR420A) on an ABI 7300 Real-Time PCR system. The primer sequences for the detection of target genes are acquired from online resource: https://pga.mgh.harvard.edu/primerbank/. Mouse *Il-36γ* primers: forward-5′-TCCTGACTTTGGGGAGGTTTT-3′; reverse-5′-TCACGCTGACTGGGGTTACT-3′. Mouse *Cxcl10* primers: forward-5′-

CCAAGTGCTGCCGTCATTTTC-3′; reverse-5′-GGCTCGCAGGGATGATTTCAA-3′. Mouse *Mst1* primers: forward-5′-CTCACCACTGAATGACTTCCAG-3′; reverse-5′-AAGGCCCGACAGTCCAGAA-3′. Mouse *Nos2* primers: forward-5′-GTTCTCAGCCCAACAATACAAGA-3′; reverse-5′-GTGGACGGGTCGATGTCAC-3′. Mouse *Arg1* primers: forward-5′-CTCCAAGCCAAAGTCCTTAGAG-3′; reverse-5′-AGGAGCTGTCATTAGGGACATC-3′. Mouse *Il-36R* primers: forward-5′-GCAGCAGATACGTGTGAGGAC-3′; reverse-5′-GTACCATGTCAGATTTACTGCCC-3′. Mouse *Caspase-1* primers: forward-5′-ACAAGGCACGGGACCTATG-3′; reverse-5′-TCCCAGTCAGTCCTGGAAATG-3′. Mouse *Gapdh* primers: forward-5′-AGGTCGGTGTGAACGGATTTG-3′; reverse-5′-TGTAGACCATGTAGTTGAGGTCA-3′. Human *IL-36α* primers: forward-5′-CCAGACGCTCATAGCAGTCC-3′; reverse-5′-AGATGGGGTTCCCTCTGTCTT-3′. Human *GAPDH* primers: forward-5′-GGAGCGAGATCCCTCCAAAAT-3′; reverse-5′-GGCTGTTGTCATACTTCTCATGG-3′.

Western blotting

Total cell lysates were equally loaded on 8-12% SDS-polyacrylamide gel for running and then transferred to PVDF membranes (GE Healthcare Life Science; 10600023). After blocking with 5% nonfat milk in TBST, the membranes were incubated for 2 hours or overnight with the primary antibodies. After staining with horseradish perioxidase (HRP)-linked secondary antibodies, signal detection was performed using a chemiluminescence phototope-HRP Kit (Millipore; WBKLS0500). p65 (8242S), p-p65 (3033S), actin (3700S), anti-mouse IgG, HRP-linked antibody (7076S) and anti-rabbit IgG, HRP-linked antibody (7074S) were purchased from Cell Signaling Technology. Caspase-1 antibody (Santa Cruz Biotechnology; sc-56036). IL-36α antibody (R&D Systems; MAB1078).

Chromatin immunoprecipitation (ChIP)

ChIP assays were performed essentially as previously described (*45*). Briefly, cells were harvested and crosslinked with 1% formaldehyde for 10 minutes at room temperature. After sonication, the soluble chromatins were incubated with the following antibodies separately: anti-H3K27me3 (Abcam; ab6002); anti-H3K4me3 (Abcam; ab8580), anti-NF-κB p65 (Santa Cruz; sc-8008) or anti-control IgG (Abcam; ab172730). Chromatin immunocomplexes were then precipitated with Protein A (Millipore; 16-661) or Protein G (Millipore; 16-662). The immunoprecipitated complex was washed, and DNA was extracted and purified by QIAquick PCR Purification Kit (Qiagen; 28104). ChIP DNA was analyzed by qPCR using specific primers, and the data were normalized by input DNA. The primers used for ChIP-qPCR were as follows: mouse *Il-36γ* for H3K27me3 or H3K4me3 binding: forward-5'-TTAGCCCTGACCCTAATCGC-3', reverse-5'-GGGAGAGAGCAGGGTAAGTG-3'; mouse *Il-36γ* for p65 binding: forward-5'-CGGAAATTTGGGGGTCTAAC-3', reverse-5'-CAGCCCCATAGGTCAGTCAC-3'. Human *IL-36α* for p65 binding: forward-5'-TCATTGACCCGGAAGAAGTC -3', reverse-5'- TGAAACATGAGGGCATGCTA-3'.

Bioinformatics analyses

HemaExplorer database was used to retrieve mRNA expression data for the expression patterns of *IL-36α* in in AML patients and normal hematopoietic cells (http://servers.binf.ku.dk/hemaexplorer) (*46*, *47*). p65 ChIP-seq data for mouse macrophages were obtained from ref. (*48*) (GEO accession: GSE46494). p65 ChIP-seq data for human aortic endothelial cells were obtained from ref. (*49*) (GEO accession: GSE89970). ChIP-seq data were processed by Cistrome analysis pipeline and was loaded to UCSC genome browsers for visualization (*50*). The microarray expression data in the BM mononuclear cells of 494 AML

patients were obtained from the GEO GSE131559 dataset (*35, 36*), the RSEM expression estimates normalized to set the upper quartile count at 1,000 for gene level and then with $\log_2$ transformation. The AML samples were clustered using the MDSC genes into MDSC-high, MDSC-low, and MDSC-medium (distance between pairs of samples was measured by Manhattan distance, and clustering was then performed using complete-linkage hierarchical clustering). Wilcoxon test was used to compare the expression of *IL-36α* in different groups.

Flow cytometry analysis and sorting

For assessing cell cycle, Ki-67 staining (BD Biosciences; 561126) were measured. For assessing cell survival, Annexin V-APC/BV421 staining (BD Biosciences; 550474/563973) were measured. For assessing active caspase-1, FLICA 660 Caspase-1 Assay (ImmunoChemistry Technologies; 9122) were conducted according to the manufacturers' instructions. Anti-mouse flow cytometry antibody were purchased from BD Biosciences: CD45.1-BV605/APC (747743/561873), CD45.2-APC (558702), CD8α-PE-Cy7/PerCP (552877/553036), IFN-γ-BV786 (563773), CD3e-PE/biotin/APC-Cy7/BV421 (553063/553060/557596/562600), PD-L1-BV421 (564716), c-Kit-APC/PE-Cy7 (553356/558163), Gr-1-APC/biotin/PE/BV421/PerCP-Cy5.5/FITC (553129/51-01212J/553128/562709/552093/553126), CD115-PE/APC (565249/567027), B220-biotin (553085), Ter119-biotin/BV421 (553672/563998), CD11b-biotin (51-01712J), F4/80-APC/PE (566787/565410), CD4-BV421 (562891), FOXP3-PE (560408), NK1.1-PE (553165), CD335-PE (560757). Anti-human flow cytometry antibody were purchased from BD Biosciences: CD3-APC (555342), CD8-BV786 (563823), CD34-FITC (555821), CD45-FITC (555482), CD24-PE (555428), CD56-PE-Cy7 (557747), CD14-BV421 (563743), CD16-APC (561304), CD33-APC (551378). Streptavidin BV421/PCP5.5/FITC (563259/551419/554060). APC-conjugated α-$OVA_{257-264}$ (SIINFEKL) peptide bound to H-$2K^b$

(17-5743-80) was purchased from eBioscience. APC-conjugated H-2K^{b} OVA Tetramer-SIINFEKL (TS-M008-2) was purchased from MBL. APC-conjugated anti-mouse H-2K^{b} (116518) was purchased from BioLegend. The flow cytometric data were collected with a BD Calibur or LSRII (Becton Dickinson) and analyzed using FlowJo software. In the sorting experiment, the stained cells were sorted out with a cell sorter (BD FACSAriaTM).

Fig. S1.

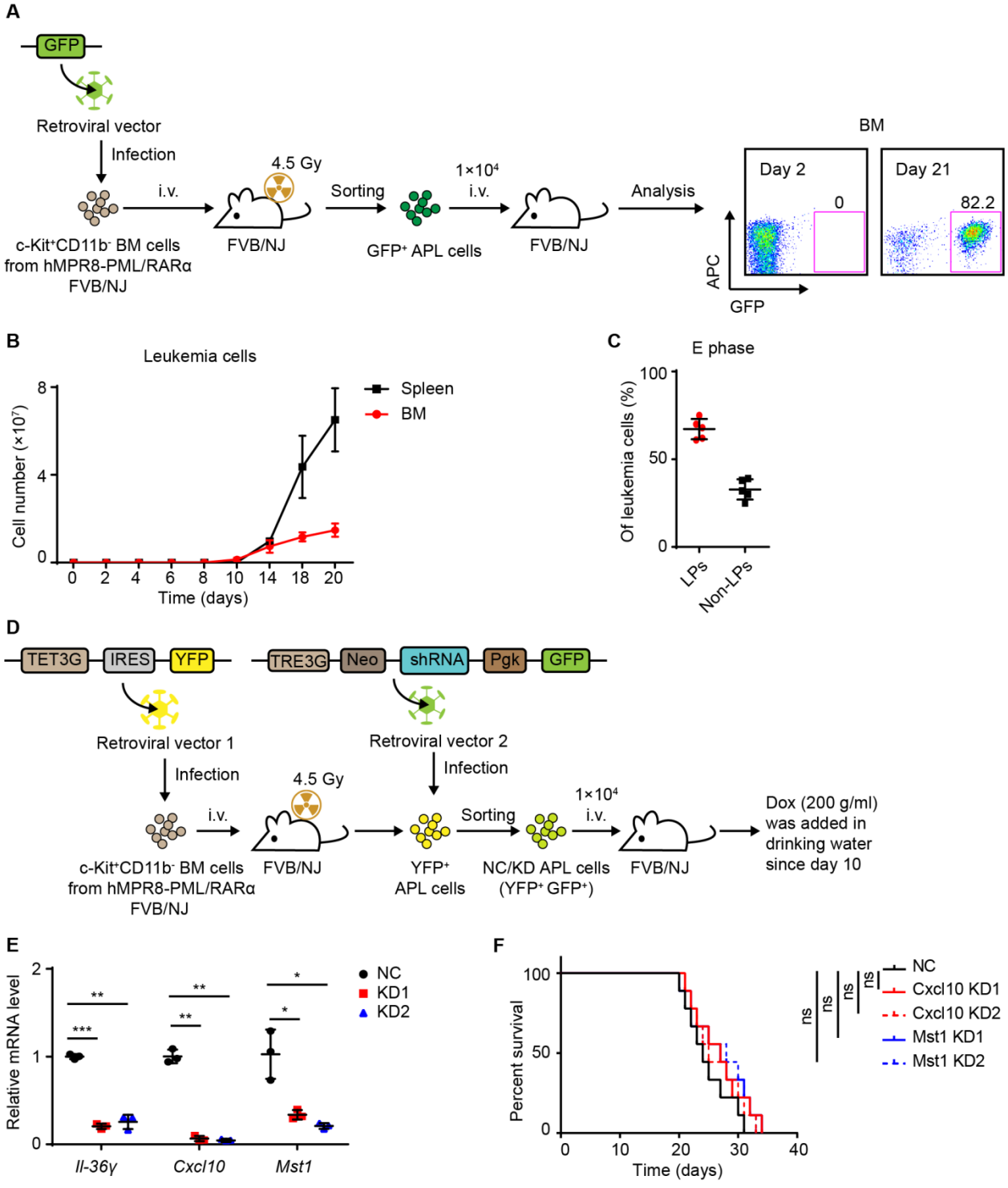
A
GFP
Retroviral vector
Infection
i.v.
4.5 Gy
Sorting
1×10⁴
i.v.
Analysis
c-Kit⁺CD11b⁻ BM cells
from hMPR8-PML/RARα
FVB/NJ
FVB/NJ
GFP⁺ APL cells
FVB/NJ
BM
Day 2
0
Day 21
82.2
APC
GFP
B
Leukemia cells
Spleen
BM
Cell number (×10⁷)
Time (days)
C
E phase
Of leukemia cells (%)
LPs
Non-LPs
D
TET3G
IRES
YFP
TRE3G
Neo
shRNA
Pgk
GFP
Retroviral vector 1
Retroviral vector 2
Infection
Infection
4.5 Gy
i.v.
Sorting
1×10⁴
i.v.
c-Kit⁺CD11b⁻ BM cells
from hMPR8-PML/RARα
FVB/NJ
FVB/NJ
YFP⁺
APL cells
NC/KD APL cells
(YFP⁺ GFP⁺)
FVB/NJ
Dox (200 g/ml)
was added in
drinking water
since day 10
E
Relative mRNA level
NC
KD1
KD2
Il-36γ
Cxcl10
Mst1
F
Percent survival
Time (days)
ns
NC
Cxcl10 KD1
Cxcl10 KD2
Mst1 KD1
Mst1 KD2

Fig. S1. Leukemic Il-36γ but not Cxcl10 or Mst1 promotes leukemic progression.

(A-C) The c-Kit$^+$CD11b$^-$ BM cells from *hMRP8-PML-RARα* transgenic FVB/NJ mice were infected with retroviral MigR1 vector expressing GFP and transplanted into sub-lethally irradiated (4.5 Gy) FVB/NJ mice. Then, 1×10^4 GFP$^+$ APL cells sorted from these mice were transplanted into non-irradiated FVB/NJ mice to establish APL model **(A)**. **(B)** The numbers of APL cells in BM and spleen are shown (n=5 mice per time points). **(C)** The percentages of LPs (c-Kit$^+$) and non-LPs (c-Kit$^-$) in BM APL cells during the E phase are shown (n=5 mice).

(D-F) Flow chart **(D)** of the genetic incorporation of Dox-inducible expression system into APL cells. Retroviral vector 1 contained the expression cassette of TET3G and YFP. Retroviral vector 2 contained an expression cassette of the negative control (NC) or knockdown (KD) shRNA under the direction of Dox responsive TRE3G, and a separate GFP expression cassette under the direction of Pgk promoter. After infection, 1×10^4 YFP$^+$GFP$^+$ NC or KD APL cells were sorted and transplanted into non-irradiated FVB/NJ mice to establish the APL mice model. Dox was supplied since day 10. **(E)** qRT-PCR analysis for the mRNA level of knockdown genes in BM APL cells treated with Dox for 6 days *in vivo* (n=3). **(F)** Survival curve of the APL recipients were generated (n=9 mice per group).

Data are presented as mean ± SD. *$p < 0.05$, **$p < 0.01$, ***$p < 0.001$. ns: not significant.

Fig. S2.

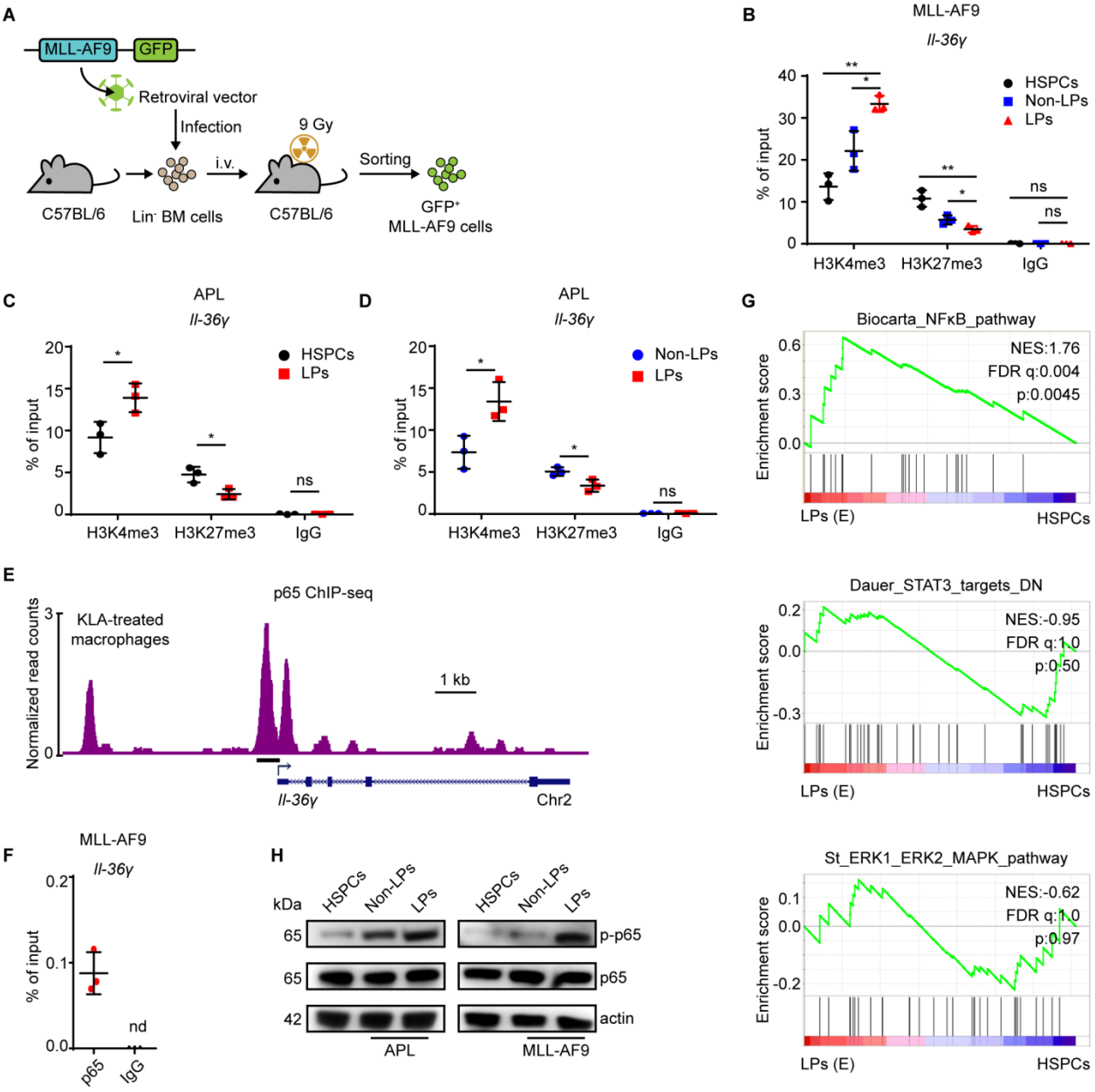
A
MLL-AF9
GFP
Retroviral vector
Infection
9 Gy
i.v.
Sorting
C57BL/6
Lin- BM cells
C57BL/6
GFP+
MLL-AF9 cells
B
MLL-AF9
Il-36γ
% of input
HSPCs
Non-LPs
LPs
H3K4me3
H3K27me3
IgG
ns
C
APL
Il-36γ
HSPCs
LPs
D
APL
Il-36γ
Non-LPs
LPs
E
p65 ChIP-seq
KLA-treated macrophages
Normalized read counts
1 kb
Il-36γ
Chr2
F
MLL-AF9
Il-36γ
nd
p65
IgG
G
Biocarta_NFκB_pathway
NES:1.76
FDR q:0.004
p:0.0045
Enrichment score
LPs (E)
HSPCs
Dauer_STAT3_targets_DN
NES:-0.95
FDR q:1.0
p:0.50
St_ERK1_ERK2_MAPK_pathway
NES:-0.62
FDR q:1.0
p:0.97
H
kDa
HSPCs
Non-LPs
LPs
p-p65
p65
actin
APL
MLL-AF9

Fig. S2. NF-κB pathway activates *Il-36γ* expression in the AML LPs.

(A) Retroviral vector contained the expression cassette of MLL-AF9 and GFP infected lineage$^-$ BM cells from C57BL/6 mice. Then, these cells were transplanted into lethally irradiated (9 Gy) C57BL/6 mice. When these recipients were moribund, BM GFP$^+$ MLL-AF9 cells were sorted for experiments.

(B-D) ChIP-qPCR assay for H3K4me3 and H3K27me3 levels at a potential regulatory element of *Il-36γ* locus in HSPCs, LPs and non-LPs (n=3).

(E-F) ChIP-seq occupancy profiles of p65 at *Il-36γ* gene locus in KLA-treated mouse macrophages, and the underline indicates the location of the p65-binding site used for ChIP-qPCR analysis **(E)**. **(F)** ChIP-qPCR assay for p65 or IgG occupancy at the *Il-36γ* locus in the LPs (n=3).

(G) GSEA analysis of NF-κB, STAT3 and ERK pathways in APL LPs versus HSPCs.

(H) Western blot analysis of phosphorylated-p65 (p-p65) and p65 levels in HSPCs, LPs and non-LPs of two AML models.

Data are presented as mean ± SD. *$p < 0.05$, **$p < 0.01$. ns: not significant. nd: not detected.

Fig. S3.

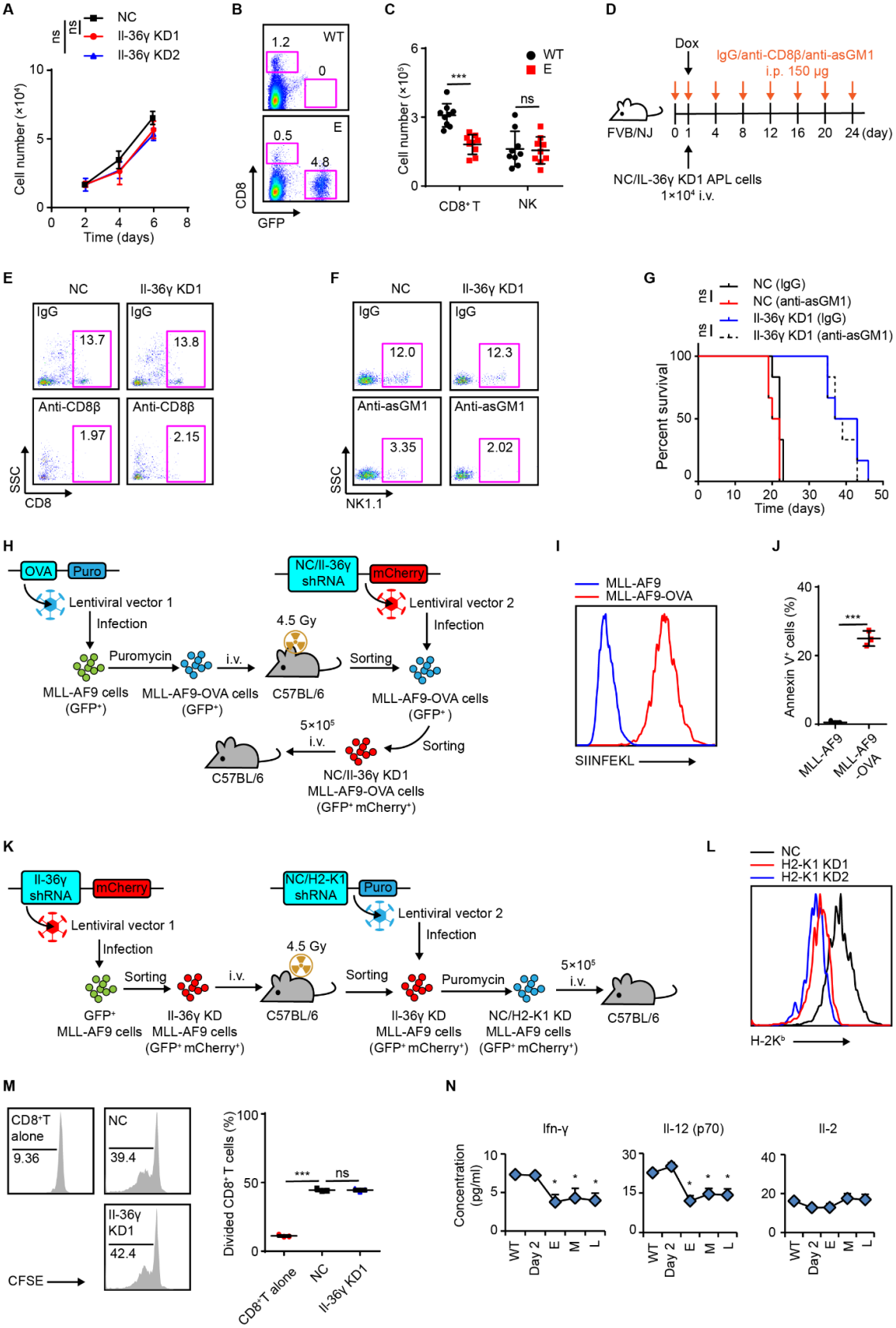
A
NC
Il-36γ KD1
Il-36γ KD2
ns
Cell number (×10⁴)
Time (days)
B
WT
E
1.2
0
0.5
4.8
CD8
GFP
C
WT
E
***
ns
Cell number (×10⁵)
CD8⁺T
NK
D
Dox
IgG/anti-CD8β/anti-asGM1
i.p. 150 μg
FVB/NJ
0 1 4 8 12 16 20 24 (day)
NC/IL-36γ KD1 APL cells
1×10⁴ i.v.
E
NC
Il-36γ KD1
IgG
13.7
13.8
Anti-CD8β
1.97
2.15
SSC
CD8
F
NC
Il-36γ KD1
IgG
12.0
12.3
Anti-asGM1
3.35
2.02
SSC
NK1.1
G
NC (IgG)
NC (anti-asGM1)
Il-36γ KD1 (IgG)
Il-36γ KD1 (anti-asGM1)
ns
Percent survival
Time (days)
H
OVA
Puro
Lentiviral vector 1
Infection
Puromycin
MLL-AF9 cells
(GFP⁺)
i.v.
MLL-AF9-OVA cells
(GFP⁺)
C57BL/6
4.5 Gy
NC/Il-36γ
shRNA
mCherry
Lentiviral vector 2
Infection
Sorting
MLL-AF9-OVA cells
(GFP⁺)
5×10⁵
i.v.
C57BL/6
Sorting
NC/Il-36γ KD1
MLL-AF9-OVA cells
(GFP⁺ mCherry⁺)
I
MLL-AF9
MLL-AF9-OVA
SIINFEKL
J
Annexin V⁺ cells (%)
***
MLL-AF9
MLL-AF9-OVA
K
Il-36γ
shRNA
mCherry
Lentiviral vector 1
Infection
Sorting
GFP⁺
MLL-AF9 cells
i.v.
Il-36γ KD
MLL-AF9 cells
(GFP⁺ mCherry⁺)
C57BL/6
4.5 Gy
NC/H2-K1
shRNA
Puro
Lentiviral vector 2
Infection
Sorting
Il-36γ KD
MLL-AF9 cells
(GFP⁺ mCherry⁺)
Puromycin
NC/H2-K1 KD
MLL-AF9 cells
(GFP⁺ mCherry⁺)
5×10⁵
i.v.
C57BL/6
L
NC
H2-K1 KD1
H2-K1 KD2
H-2Kᵇ
M
CD8⁺T
alone
9.36
NC
39.4
Il-36γ
KD1
42.4
CFSE
Divided CD8⁺T cells (%)
***
ns
CD8⁺T alone
NC
Il-36γ KD1
N
Ifn-γ
Il-12 (p70)
Il-2
Concentration
(pg/ml)
WT
Day 2
E
M
L

Fig. S3. Il-36γ supports leukemic progression by restraining $CD8^+$ T cell-mediated immunorejection.

(A) 1×10^4 APL LPs were treated with Dox (1 μg/ml) *in vitro*. The numbers of LPs were counted (n=3).

(B-C) WT FVB/NJ mice and APL mice in the E phase were sacrificed. The representative cytometric profile of BM **(B)**, the number of $CD8^+$ T ($CD3^+CD8^+$) and NK ($CD3^-Nk1.1^+$) **(C)** in BM were measured (n=9 mice per group).

(D-G) 1×10^4 NC or Il-36γ KD APL cells were inoculated into non-irradiated FVB/NJ and treated with IgG, anti-asGM1 or anti-CD8β (i.p. 150 μg) at indicated days. Dox was given immediately after transplantation **(D)**. Representative flow plots showed the percentages of $CD8^+$ T **(E)** or NK **(F)** in the PB of the recipients after having been treated with different antibody as indicated. **(G)** Survival curves of the recipients were generated (n=6 mice per group).

(H-J) Lentiviral vector 1 containing the expression cassettes of OVA and Puro infected GFP^+ BM MLL-AF9 cells. After puromycin selection, these cells were transplanted into sub-lethally irradiated (4.5 Gy) C57BL/6 mice. Then, GFP^+ MLL-AF9-OVA cells were sorted from these recipients and infected with NC or Il-36γ KD lentiviral vector 2. After infection, 5×10^5 NC or Il-36γ KD MLL-AF9-OVA cells ($GFP^+mCherry^+$) were transplanted into non-irradiated C57BL/6 mice to establish the leukemic model **(H)**. **(I)** The presentation of OVA-derived SIINFEKL peptide by $H\text{-}2K^b$ in MLL-AF9 cells or MLL-AF9-OVA cells was analyzed by flow cytometry. **(J)** Splenocytes from the OT-1 transgenic mice were cultured with SIINFEKL peptide (7.5 μg/ml) for 5 days. Then, $CD8^+$ T cells were purified and cultured with MLL-AF9 cells or MLL-AF9-OVA cells at 8:1 ratio for 4 hours. After culture, leukemia cells were assessed for Annexin V staining (n=3).

(K-L) Lentiviral vector 1 containing the expression cassettes of Il-36γ KD shRNA and mCherry infected GFP^+ BM MLL-AF9 cells. After sorting, $GFP^+mCherry^+$ Il-36γ KD MLL-AF9 cells were transplanted into sub-irradiated (4.5 Gy) C57BL/6 mice. Then, $GFP^+mCherry^+$ Il-36γ KD MLL-AF9 cells isolated from these recipients were infected with NC or H2-K1 KD lentiviral vector 2. After puromycin selecting, 5×10^5 NC or H2-K1 KD cells were transplanted into non-irradiated C57BL/6 mice for survival analysis **(K)**. **(L)** NC or H2-K1 KD MLL-AF9 cells were tested for $H2\text{-}K^b$ expression.

(M) Spleen $CD8^+$ T cells from FVB/NJ mice stained with CFSE were cultured alone or cultured with NC or Il-36γ KD APL cells at 16:1 ratio in 96-well plates coated with anti-CD3 for 3 days. Dox (1 μg/ml) were added. The proliferation of T cells was assayed by monitoring CFSE intensity (n=3).

(N) The protein levels of Ifn-γ, Il-12 (p70) and Il-2 in BM along with APL progression were assayed by cytokine array (n=8 mice per group).

Data are presented as mean ± SD. $*p < 0.05$, $***p < 0.001$. ns: not significant.

Fig. S4.

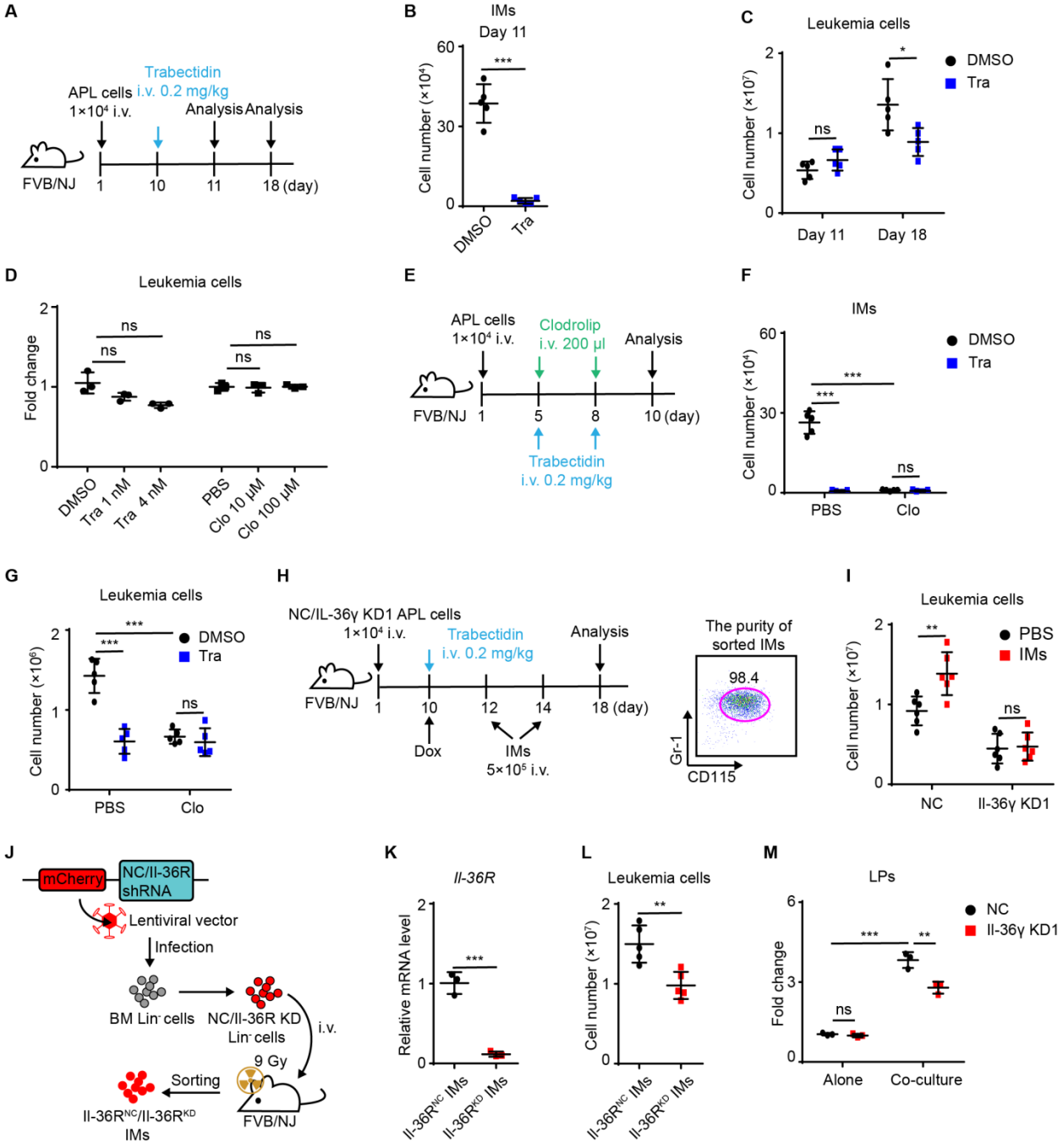
A
Trabectidin
APL cells i.v. 0.2 mg/kg
1×10⁴ i.v.
Analysis Analysis
FVB/NJ
1
10
11
18 (day)
B
IMs
Day 11
Cell number (×10⁴)
***
DMSO
Tra
C
Leukemia cells
Cell number (×10⁷)
*
ns
DMSO
Tra
Day 11
Day 18
D
Leukemia cells
Fold change
ns
DMSO
Tra 1 nM
Tra 4 nM
PBS
Clo 10 μM
Clo 100 μM
E
APL cells
1×10⁴ i.v.
Clodrolip
i.v. 200 μl
Analysis
FVB/NJ
10 (day)
Trabectidin
i.v. 0.2 mg/kg
F
IMs
Cell number (×10⁴)
DMSO
Tra
PBS
Clo
G
Leukemia cells
Cell number (×10⁶)
DMSO
Tra
PBS
Clo
H
NC/IL-36γ KD1 APL cells
1×10⁴ i.v.
Trabectidin
i.v. 0.2 mg/kg
Analysis
FVB/NJ
18 (day)
Dox
IMs
5×10⁵ i.v.
The purity of
sorted IMs
98.4
Gr-1
CD115
I
Leukemia cells
Cell number (×10⁷)
PBS
IMs
NC
Il-36γ KD1
J
mCherry
NC/Il-36R
shRNA
Lentiviral vector
Infection
BM Lin⁻ cells
NC/Il-36R KD
Lin⁻ cells
i.v.
9 Gy
Sorting
Il-36R^NC/Il-36R^KD
IMs
FVB/NJ
K
Il-36R
Relative mRNA level
Il-36R^NC IMs
Il-36R^KD IMs
L
Leukemia cells
Cell number (×10⁷)
Il-36R^NC IMs
Il-36R^KD IMs
M
LPs
Fold change
NC
Il-36γ KD1
Alone
Co-culture

Fig. S4. Il-36γ-activated IMs promote leukemic progression.

(A-C) Scheme **(A)** for trabectedin treatment to APL mice. The numbers of IMs **(B)** and APL cells **(C)** in BM were counted at indicated time points (n=5 mice per group).

(D) APL cells were treated with different concentrations of trabectedin or clodrolip for 3 days *in vitro*. Histogram shows the relative numbers of APL cells (n=3).

(E-G) Scheme **(E)** for trabectedin and/or clodrolip treatment to APL mice. **(F-G)** The numbers of IMs and leukemia cells in BM at day 10 are shown (n=5 mice per group).

(H-I) 1×10^4 NC or Il-36γ KD APL cells were inoculated into non-irradiated FVB/NJ mice. Trabectedin was injected at day 10. Dox was supplied since day 10. Then, PBS or 5×10^5 IMs sorted from WT FVB/NJ mice were inoculated into these APL mice at day 12 and day 14 **(H)**. **(I)** The numbers of APL cells in BM of different groups at day 18 were measured (n=6 mice per group).

(J-L) FVB/NJ mice-derived BM lineage$^-$ cells infected with lentiviral vector expressing Il-36R shRNA were transplanted into lethally irradiated (9 Gy) FVB/NJ mice **(J)**. **(K)** qRT-PCR analysis of *Il-36R* mRNA level in IMs isolated from the chimeric mice (n=3). **(L)** 1×10^4 NC APL cells were inoculated into non-irradiated FVB/NJ mice. Trabectedin was injected at day 10. Dox was supplied since day 10. Then, 5×10^5 IMs isolated from Il-36R^{NC} or Il-36R^{KD} chimeric mice were inoculated into these APL mice at day 12 and day 14. The numbers of APL cells in BM of different groups at day 18 were measured (n=5 mice per group).

(M) APL LPs were cultured alone or cultured with IMs at 1:10 ratio for 3 days *in vitro*. Dox (1 μg/ml) was added. Histograms show the relative numbers of the LPs after culture (n=3).

Data are presented as mean ± SD. *$p < 0.05$, **$p < 0.01$, ***$p < 0.001$. ns: not significant.

Fig. S5.

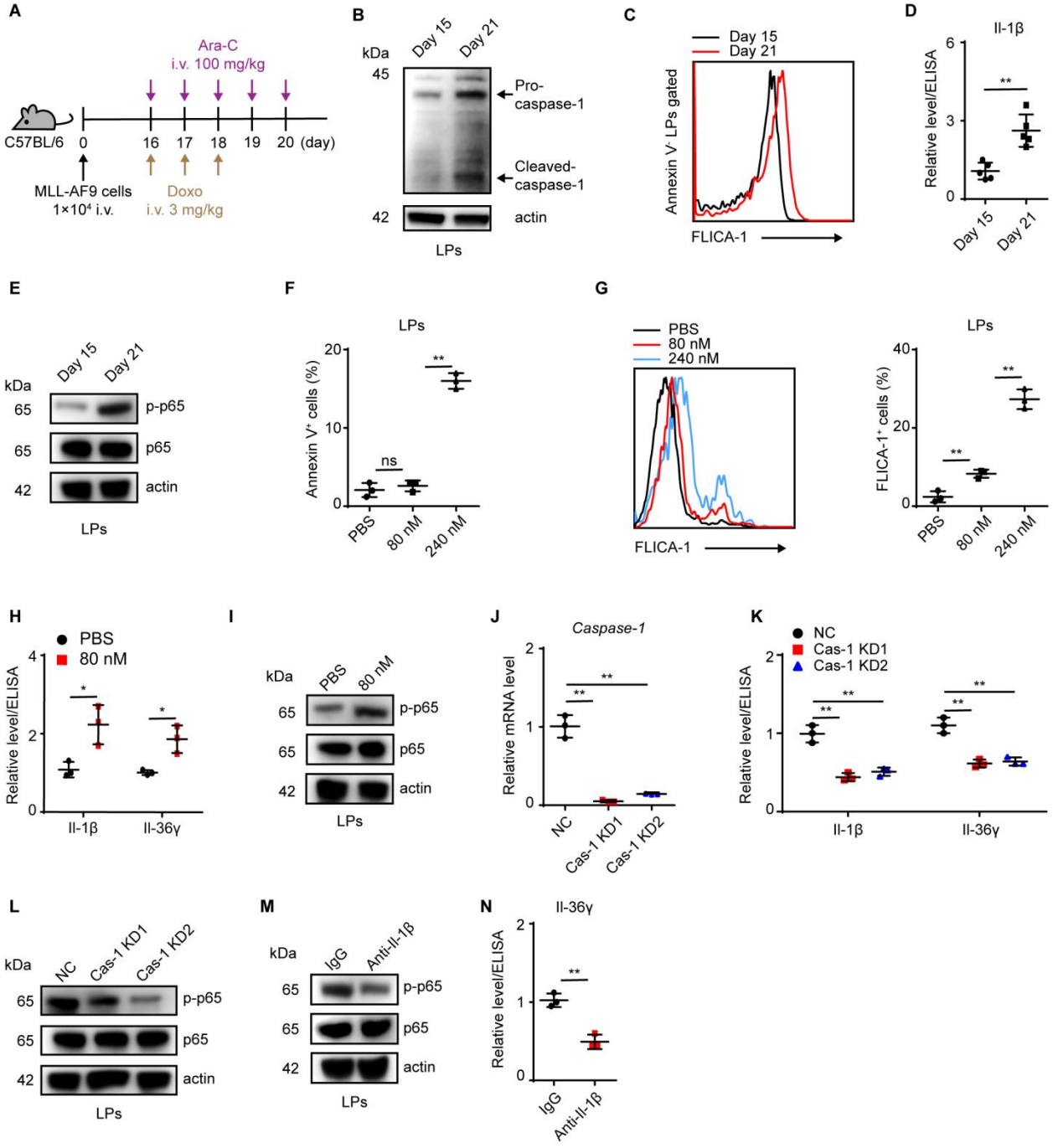
A
Ara-C
i.v. 100 mg/kg
C57BL/6
0
16
17
18
19
20 (day)
MLL-AF9 cells
1×10⁴ i.v.
Doxo
i.v. 3 mg/kg
B
kDa
Day 15
Day 21
45
Pro-caspase-1
Cleaved-caspase-1
42
actin
LPs
C
Day 15
Day 21
Annexin V⁻ LPs gated
FLICA-1
D
Il-1β
Relative level/ELISA
Day 15
Day 21
E
kDa
Day 15
Day 21
65
p-p65
65
p65
42
actin
LPs
F
LPs
Annexin V⁺ cells (%)
ns
PBS
80 nM
240 nM
G
PBS
80 nM
240 nM
FLICA-1
LPs
FLICA-1⁺ cells (%)
H
PBS
80 nM
Relative level/ELISA
Il-1β
Il-36γ
I
kDa
PBS
80 nM
p-p65
p65
actin
LPs
J
Caspase-1
Relative mRNA level
NC
Cas-1 KD1
Cas-1 KD2
K
NC
Cas-1 KD1
Cas-1 KD2
Relative level/ELISA
Il-1β
Il-36γ
L
kDa
NC
Cas-1 KD1
Cas-1 KD2
p-p65
p65
actin
LPs
M
kDa
IgG
Anti-Il-1β
p-p65
p65
actin
LPs
N
Il-36γ
Relative level/ELISA
IgG
Anti-Il-1β

Fig. S5. Caspase-1-Il-1β-NF-κB axis in AML LPs mediates Il-36γ upregulation after chemotherapy.

(A-E) Scheme for the AD regimen in MLL-AF9 mice model **(A)**. **(B)** Western blot assay on the expression of caspase-1 in BM LPs at the indicated days. **(C)** Representative flow cytometric analyses of activated caspase-1 in Annexin V^- BM LPs isolated at the indicated days. **(D)** BM LPs were sorted at indicated days (n=5 mice per group) and cultured *in vitro* for 3 days. Then, the relative Il-1β level in culture medium were measured by ELISA. **(E)** Western blot assay on the expression of p-p65 in BM LPs isolated at the indicated time points.

(F-I) MLL-AF9 LPs were treated with PBS or Ara-C for 48 hours *in vitro*. Cell death **(F)** and caspase-1 activation **(G)** were measured using Annexin V staining and FLICA-1 fluorescent probes (n=3). **(H)** The relative levels of Il-1β and Il-36γ in culture medium were measured by ELISA (n=3). **(I)** The levels of p-p65 were measured by western blot.

(J-L) NC or Caspase-1 KD MLL-AF9 LPs were treated with Ara-C (80 nM) for 48 hours *in vitro*. **(J)** qRT-PCR analysis of *Caspase-1* mRNA level as indicated (n=3). **(K)** The levels of Il-1β and Il-36γ in culture medium were measured by ELISA (n=3). **(L)** The levels of p65 and p-p65 were measured by western blot.

(M-N) MLL-AF9 LPs were treated with Ara-C (80 nM) for 48 hours in presence of IgG or anti-Il-1β antibody (100 μg/ml) *in vitro*. **(M)** The levels of p65 and p-p65 were measured by western blot. **(N)** The level of Il-36γ in culture medium was measured by ELISA (n=3).

Data are presented as mean ± SD. $*p < 0.05$, $**p < 0.01$. ns: not significant.

Fig. S6.

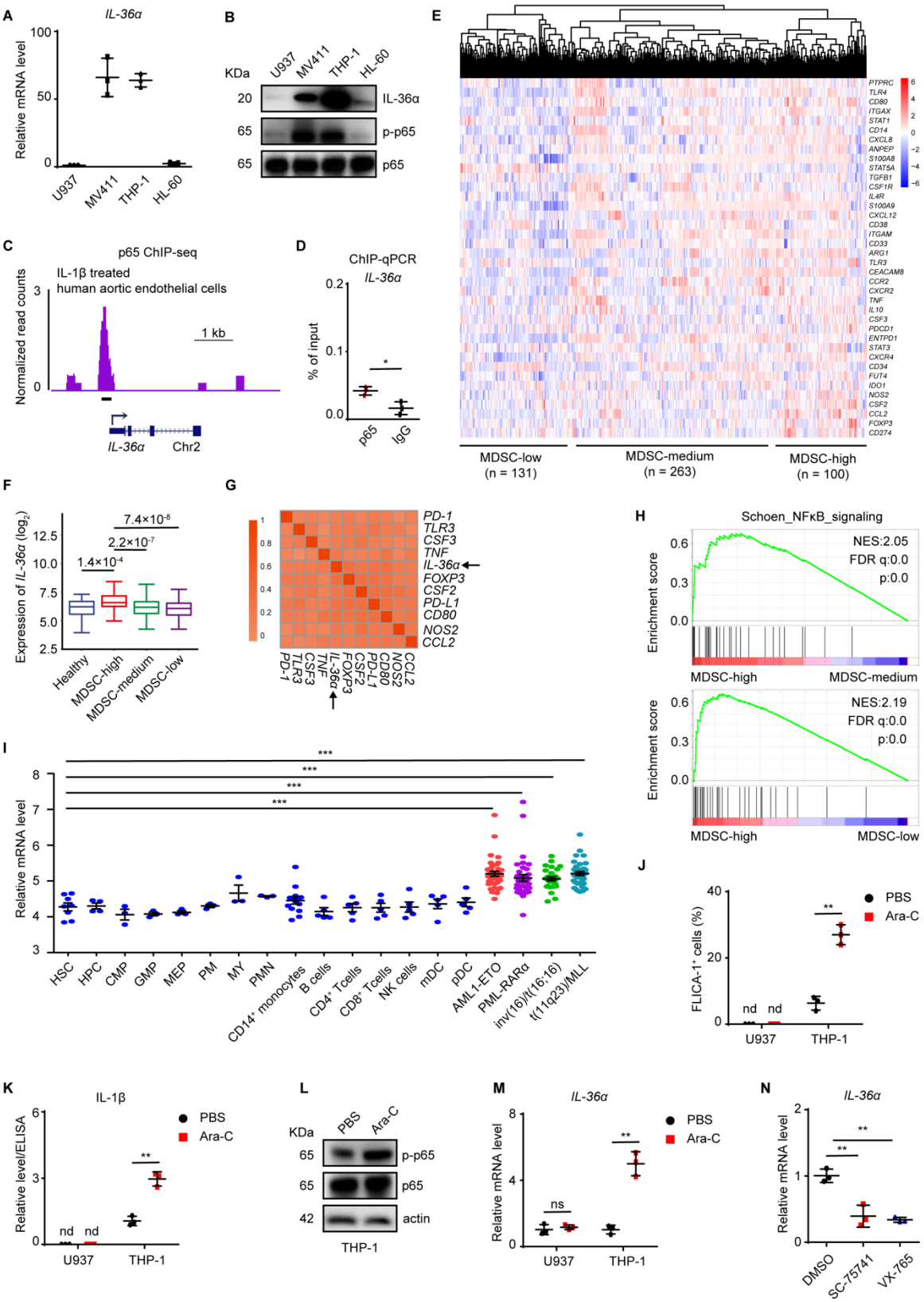
A
IL-36α
Relative mRNA level
U937
MV411
THP-1
HL-60
B
KDa
IL-36α
p-p65
p65
C
p65 ChIP-seq
IL-1β treated
human aortic endothelial cells
Normalized read counts
1 kb
IL-36α
Chr2
D
ChIP-qPCR
IL-36α
% of input
p65
IgG
E
MDSC-low
(n = 131)
MDSC-medium
(n = 263)
MDSC-high
(n = 100)
F
Expression of IL-36α (log2)
Healthy
MDSC-high
MDSC-medium
MDSC-low
G
PD-1
TLR3
CSF3
TNF
IL-36α
FOXP3
CSF2
PD-L1
CD80
NOS2
CCL2
H
Schoen_NFκB_signaling
NES:2.05
FDR q:0.0
p:0.0
MDSC-high
MDSC-medium
NES:2.19
FDR q:0.0
p:0.0
MDSC-high
MDSC-low
I
Relative mRNA level
HSC
HPC
CMP
GMP
MEP
PM
MY
PMN
CD14+ monocytes
B cells
CD4+ Tcells
CD8+ Tcells
NK cells
mDC
pDC
AML1-ETO
PML-RARα
inv(16)/t(16;16)
t(11q23)/MLL
J
FLICA-1+ cells (%)
PBS
Ara-C
nd
nd
U937
THP-1
K
IL-1β
Relative level/ELISA
PBS
Ara-C
nd
nd
U937
THP-1
L
KDa
PBS
Ara-C
p-p65
p65
actin
THP-1
M
IL-36α
Relative mRNA level
PBS
Ara-C
ns
U937
THP-1
N
IL-36α
Relative mRNA level
DMSO
SC-75741
VX-765

Fig. S6. IL-36α is upregulated in human AML blasts.

(A) qRT-PCR assay on the mRNA levels of *IL-36α* in human leukemia cell lines (n=3).

(B) The levels of p-p65, p65 and IL-36α in human leukemia cell lines were measured by western blot.

(C-D) ChIP-seq occupancy profiles of the NF-κB p65 at *Il-36α* gene locus in IL-1β-treated human aortic endothelial cells, and the underline indicates the location of binding sequence used for ChIP-qPCR analysis **(C)**. **(D)** ChIP-qPCR assay for p65 or IgG occupancy at the *Il-36α* locus in THP-1 cells (n=3).

(E-H) Unsupervised clustering of 494 human AML samples into MDSC-high, MDSC-low and MDSC-medium groups using a 39-gene MDSC signature **(E)**. **(F)** *IL-36α* mRNA levels in healthy and three groups of AML samples. **(G)** Pearson correlation analysis identified top ten MDSC signature genes highly correlated with the *IL-36α* expression among 494 AML samples. **(H)** GSEA shows that the expression of signature genes of NF-κB pathway was more enriched in the MDSC-high group compared to the MDSC-medium or MDSC-low group.

(I) Analysis of *IL-36α* mRNA level in BM HSC (hematopoietic stem cells), HPC (hematopoietic progenitor cells), CMP (common myeloid progenitors), GMP (granulocyte monocyte progenitors), MEP (megakaryocyte erythroid progenitors), PM (promyelocyte), MY (myelocyte), PMN (polymorphonuclear cells), $CD14^+$ monocytes, B cells, $CD4^+$ T cells, $CD8^+$ T cells, NK cells, mDC, pDC, primary AML BM blastic samples with AML1-ETO fusion protein (n=39), with PML-RARα fusion protein (n=37), with inv(16)/t(16;16) (n=28) and with t(11q23)/MLL (n=38) using HemaExplorer database. Datasets from HemaExplorer were first separated into batches according to platform and laboratory. These batches were normalized using robust multi-array average (RMA) method provided in the affy package in R. Batch effects were corrected

using ComBat.

(J-M) Leukemia cells were treated with PBS or Ara-C (200 nM) for 72 hours. The activated caspase-1 **(J)**, the p-p65 level **(L)** and the mRNA level of *Il-36α* (n=3) **(M)** in leukemia cells are shown. **(K)** The relative levels of IL-1β in culture medium were assayed by ELISA (n=3).

(N) THP-1 cells were treated with Ara-C (200 nM) in presence or absence of the inhibitor of Caspase-1 (VX-765, 100 μM) or NF-κB (SC-75741, 5 μM) for 72 hours. The mRNA level of *Il-36α* was assayed by qRT-PCR (n=3).

Data are presented as mean ± SD. *$p < 0.05$, **$p < 0.01$, ***$p < 0.001$. ns: not significant. nd: not detected.

Fig. S7.

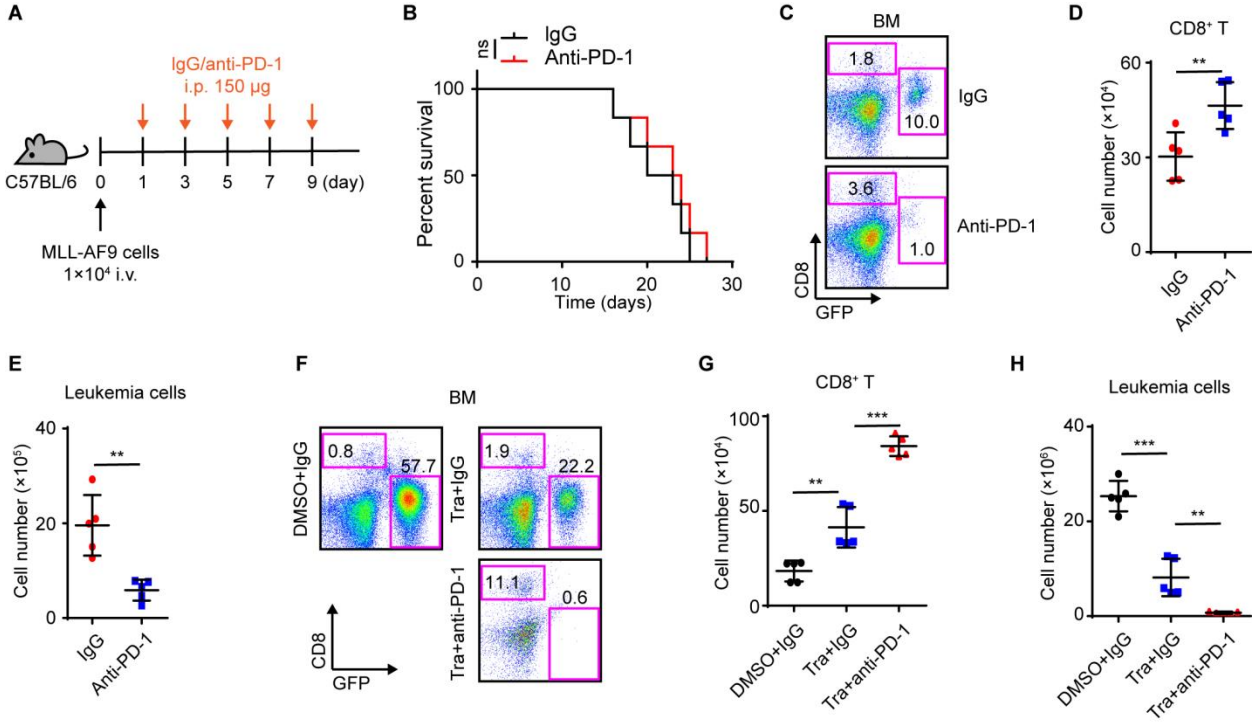
A
IgG/anti-PD-1
i.p. 150 μg
C57BL/6
0
1
3
5
7
9 (day)
MLL-AF9 cells
1×10⁴ i.v.
B
ns
IgG
Anti-PD-1
Percent survival
Time (days)
C
BM
1.8
10.0
IgG
3.6
1.0
Anti-PD-1
CD8
GFP
D
CD8⁺ T
Cell number (×10⁴)
IgG
Anti-PD-1
E
Leukemia cells
Cell number (×10⁵)
IgG
Anti-PD-1
F
BM
DMSO+IgG
0.8
57.7
Tra+IgG
1.9
22.2
Tra+anti-PD-1
11.1
0.6
CD8
GFP
G
CD8⁺ T
Cell number (×10⁴)
DMSO+IgG
Tra+IgG
Tra+anti-PD-1
H
Leukemia cells
Cell number (×10⁶)
DMSO+IgG
Tra+IgG
Tra+anti-PD-1

Fig. S7. Il-36γ knockdown or IM depletion improves the response of AML to anti-PD-1 therapy.

(A-B) Scheme for anti-PD-1 treatment to MLL-AF9 mice model **(A)**. **(B)** Survival curves of the leukemic mice (n=6 mice per group) are shown.

(C-E) 1×10^4 Il-36γ KD MLL-AF9 cells were inoculated into non-irradiated recipients and treated as described in Fig. S7A. The mice were sacrificed at day 11. The representative flow cytometric analysis of BM **(C)**, the number of T cells **(D)** and leukemia cells **(E)** in BM are shown (n=5 mice per group).

(F-H) 1×10^4 MLL-AF9 cells were inoculated into non-irradiated recipients and treated as described in Fig. S7A. DMSO or trabectadin (i.v. 0.2 mg/kg) were injected at day 1, 5, 9. The mice were sacrificed at day 15. The representative flow cytometric analysis of BM **(F)**, and the numbers of T cells **(G)** and leukemia cells **(H)** in BM are shown (n=5 mice per group).

Data are presented as mean ± SD. $^{**}p < 0.01$, $^{***}p < 0.001$. ns: not significant.

Table S1. General patient information of 15 leukemia samples used in this study.

Sample_ID in text	Age (yrs)	Gender	Specimen	FAB subtype	Index
AML#1	44	Male	BM supernatant	M0	F6A
AML#2	18	Male	BM supernatant	M2	F6A
AML#3	54	Male	BM supernatant	M2	F6A
AML#4	43	Male	BM supernatant/CM/FC	M4	F6A, F6K-M
AML#5	67	Female	BM supernatant/CM/FC/LPs RNA	M5	F6A, F6D, F6K-O
AML#6	36	Male	BM supernatant/CM/FC	M4	F6A, F6K-O
AML#7	43	Female	BM supernatant/CM/FC	M4	F6A, F6K-M
AML#8	75	Male	BM supernatant/CM/FC	M5	F6A, F6K-L
AML#9	44	Male	BM supernatant/CM/LPs RNA/Non-LPs RNA	M4	F6A, F6D-J
AML#10	50	Male	BM supernatant/LPs RNA/Non-LPs RNA/CM	M4	F6A, F6D-H
AML#11	45	Male	BM supernatant/CM/LPs RNA/Non-LPs RNA	M5	F6A, F6D-E, F6I-J
AML#12	35	Male	CM/LPs RNA/Non-LPs	M5	F6D-H

			RNA		
AML#13	63	Male	CM/FC/LPs RNA	Unclassified	F6D, F6K-L
AML#14	32	Male	CM/FC	M5	F6K-L
AML#15	71	Female	CM/FC	Non-M3	F6K-L

BM, Bone marrow; CM, Conditioned medium; FC, Flow cytometry; LPs, Leukemic progenitor cells; F, Figure.

REFERENCES AND NOTES

1. N. J. Short, S. Zhou, C. Fu, D. A. Berry, R. B. Walter, S. D. Freeman, C. S. Hourigan, X. Huang, G. Nogueras Gonzalez, H. Hwang, X. Qi, H. Kantarjian, F. Ravandi, Association of measurable residual disease with survival outcomes in patients with acute myeloid leukemia: A systematic review and meta-analysis. *JAMA Oncol.* **6**, 1890–1899 (2020).

2. M. J. Christopher, A. A. Petti, M. P. Rettig, C. A. Miller, E. Chendamarai, E. J. Duncavage, J. M. Klco, N. M. Helton, M. O'Laughlin, C. C. Fronick, R. S. Fulton, R. K. Wilson, L. D. Wartman, J. S. Welch, S. E. Heath, J. D. Baty, J. E. Payton, T. A. Graubert, D. C. Link, M. J. Walter, P. Westervelt, T. J. Ley, J. F. DiPersio, Immune escape of relapsed AML cells after allogeneic transplantation. *N. Engl. J. Med.* **379**, 2330–2341 (2018).

3. C. Toffalori, L. Zito, V. Gambacorta, M. Riba, G. Oliveira, G. Bucci, M. Barcella, O. Spinelli, R. Greco, L. Crucitti, N. Cieri, M. Noviello, F. Manfredi, E. Montaldo, R. Ostuni, M. M. Naldini, B. Gentner, M. Waterhouse, R. Zeiser, J. Finke, M. Hanoun, D. W. Beelen, I. Gojo, L. Luznik, M. Onozawa, T. Teshima, R. Devillier, D. Blaise, C. J. M. Halkes, M. Griffioen, M. G. Carrabba, M. Bernardi, J. Peccatori, C. Barlassina, E. Stupka, D. Lazarevic, G. Tonon, A. Rambaldi, D. Cittaro, C. Bonini, K. Fleischhauer, F. Ciceri, L. Vago, Immune signature drives leukemia escape and relapse after hematopoietic cell transplantation. *Nat. Med.* **25**, 603–611 (2019).

4. N. Daver, G. Garcia-Manero, S. Basu, P. C. Boddu, M. Alfayez, J. E. Cortes, M. Konopleva, F. Ravandi-Kashani, E. Jabbour, T. Kadia, G. M. Nogueras-Gonzalez, J. Ning, N. Pemmaraju, C. D. DiNardo, M. Andreeff, S. A. Pierce, T. Gordon, S. M. Kornblau, W. Flores, Z. Alhamal, C. Bueso-Ramos, J. L. Jorgensen, K. P. Patel, J. Blando, J. P. Allison, P. Sharma, H. Kantarjian, Efficacy, safety, and biomarkers of response to azacitidine and nivolumab in relapsed/refractory acute myeloid leukemia: A nonrandomized, open-label, phase II study. *Cancer Discov.* **9**, 370–383 (2019).

5. F. S. Lichtenegger, C. Krupka, S. Haubner, T. Kohnke, M. Subklewe, Recent developments in immunotherapy of acute myeloid leukemia. *J. Hematol. Oncol.* **10**, 142 (2017).

6. J. Vadakekolathu, M. D. Minden, T. Hood, S. E. Church, S. Reeder, H. Altmann, A. H. Sullivan, E. J. Viboch, T. Patel, N. Ibrahimova, S. E. Warren, A. Arruda, Y. Liang, T. H. Smith, G. A. Foulds, M. D. Bailey, J. Gowen-MacDonald, J. Muth, M. Schmitz, A. Cesano, A. G. Pockley, P. J. M. Valk, B. Löwenberg, M. Bornhäuser, S. K. Tasian, M. P. Rettig, J. K. Davidson-Moncada, J. F. DiPersio, S. Rutella, Immune landscapes predict chemotherapy resistance and immunotherapy response in acute myeloid leukemia. *Sci. Transl. Med.* **12**, eaaz0463 (2020).

7. R. P. Gale, G. Opelz, Commentary: Does immune suppression increase risk of developing acute myeloid leukemia? *Leukemia* **26**, 422–423 (2012).

8. A. M. Paczulla, K. Rothfelder, S. Raffel, M. Konantz, J. Steinbacher, H. Wang, C. Tandler, M. Mbarga, T. Schaefer, M. Falcone, E. Nievergall, D. Dörfel, P. Hanns, J. R. Passweg, C. Lutz, J. Schwaller, R. Zeiser, B. R. Blazar, M. A. Caligiuri, S. Dirnhofer, P. Lundberg, L. Kanz, L. Quintanilla-Martinez, A. Steinle, A. Trumpp, H. R. Salih, C. Lengerke, Absence of NKG2D ligands defines leukaemia stem cells and mediates their immune evasion. *Nature* **572**, 254–259 (2019).

9. P. van Galen, V. Hovestadt, M. H. Wadsworth Ii, T. K. Hughes, G. K. Griffin, S. Battaglia, J. A. Verga, J. Stephansky, T. J. Pastika, J. L. Story, G. S. Pinkus, O. Pozdnyakova, I. Galinsky, R. M. Stone, T. A. Graubert, A. K. Shalek, J. C. Aster, A. A. Lane, B. E. Bernstein, Single-cell RNA-seq reveals AML hierarchies relevant to disease progression and immunity. *Cell* **176**, 1265–1281.e24 (2019).

10. L. I. Shlush, A. Mitchell, L. Heisler, S. Abelson, S. W. K. Ng, A. Trotman-Grant, J. J. F. Medeiros, A. Rao-Bhatia, I. Jaciw-Zurakowsky, R. Marke, J. L. McLeod, M. Doedens, G. Bader, V. Voisin, C.J. Xu, J. D. McPherson, T. J. Hudson, J. C. Y. Wang, M. D. Minden, J. E. Dick, Tracing the origins of relapse in acute myeloid leukaemia to stem cells. *Nature* **547**, 104–108 (2017).

11. D. Thomas, R. Majeti, Biology and relevance of human acute myeloid leukemia stem cells. *Blood* **129**, 1577–1585 (2017).

12. C. Garlanda, C. A. Dinarello, A. Mantovani, The interleukin-1 family: Back to the future. *Immunity* **39**, 1003–1018 (2013).

13. M. S. Gresnigt, F. L. van de Veerdonk, Biology of IL-36 cytokines and their role in disease. *Semin. Immunol.* **25**, 458–465 (2013).

14. E. Y. Bassoy, J. E. Towne, C. Gabay, Regulation and function of interleukin-36 cytokines. *Immunol. Rev.* **281**, 169–178 (2018).

15. X. Wang, X. Zhao, C. Feng, A. Weinstein, R. Xia, W. Wen, Q. Lv, S. Zuo, P. Tang, X. Yang, X. Chen, H. Wang, S. Zang, L. Stollings, T. L. Denning, J. Jiang, J. Fan, G. Zhang, X. Zhang, Y. Zhu, W. Storkus, B. Lu, IL-36γ transforms the tumor microenvironment and promotes type 1 lymphocyte-mediated antitumor immune responses. *Cancer Cell* **28**, 296–306 (2015).

16. A. Carey, D. K. Edwards V, C. A. Eide, L. Newell, E. Traer, B. C. Medeiros, D. A. Pollyea, M. W. Deininger, R. H. Collins, J. W. Tyner, B. J. Druker, G. C. Bagby, S. K. McWeeney, A. Agarwal, Identification of interleukin-1 by functional screening as a key mediator of cellular expansion and disease progression in acute myeloid leukemia. *Cell Rep.* **18**, 3204–3218 (2017).

17. D. Brown, S. Kogan, E. Lagasse, I. Weissman, M. Alcalay, P. G. Pelicci, S. Atwater, J. M. Bishop, A PMLRARα transgene initiates murine acute promyelocytic leukemia. *Proc. Natl. Acad. Sci. U.S.A.* **94**, 2551–2556 (1997).

18. X. Liu, J. Chen, S. Yu, L. Yan, H. Guo, J. Dai, W. Zhang, J. Zhu, All-trans retinoic acid and arsenic trioxide fail to derepress the monocytic differentiation driver Irf8 in acute promyelocytic leukemia cells. *Cell Death Dis.* **8**, e2782 (2017).

19. B. O. Zhou, L. Ding, S. J. Morrison, Hematopoietic stem and progenitor cells regulate the regeneration of their niche by secreting Angiopoietin-1. *eLife* **4**, e05521 (2015).

20. J. L. Zhao, C. Ma, R. M. O'Connell, A. Mehta, R. DiLoreto, J. R. Heath, D. Baltimore, Conversion of danger signals into cytokine signals by hematopoietic stem and progenitor cells for regulation of stress-induced hematopoiesis. *Cell Stem Cell* **14**, 445–459 (2014).

21. M. Chapellier, P. Peña-Martínez, R. Ramakrishnan, M. Eriksson, M. S. Talkhoncheh, C. Orsmark-Pietras, H. Lilljebjörn, C. Högberg, A. Hagström-Andersson, T. Fioretos, J. Larsson, M. Järås,

Arrayed molecular barcoding identifies TNFSF13 as a positive regulator of acute myeloid leukemia-initiating cells. *Haematologica* **104**, 2006–2016 (2019).

22. H. Z. Guo, L.-T. Niu, W.-T. Qiang, J. Chen, J. Wang, H. Yang, W. Zhang, J. Zhu, S.-H. Yu, Leukemic IL-17RB signaling regulates leukemic survival and chemoresistance. *FASEB J.* **33**, 9565–9576 (2019).

23. M. L. Guzman, S. J. Neering, D. Upchurch, B. Grimes, D. S. Howard, D. A. Rizzieri, S. M. Luger, C. T. Jordan, Nuclear factor-κB is constitutively activated in primitive human acute myelogenous leukemia cells. *Blood* **98**, 2301–2307 (2001).

24. H.-P. Kuo, Z. Wang, D.-F. Lee, M. Iwasaki, J. Duque-Afonso, S. H. K. Wong, C.-H. Lin, M. E. Figueroa, J. Su, I. R. Lemischka, M. L. Cleary, Epigenetic roles of MLL oncoproteins are dependent on NF-κB. *Cancer Cell* **24**, 423–437 (2013).

25. Y. Kagoya, A. Yoshimi, K. Kataoka, M. Nakagawa, K. Kumano, S. Arai, H. Kobayashi, T. Saito, Y. Iwakura, M. Kurokawa, Positive feedback between NF-κB and TNF-α promotes leukemia-initiating cell capacity. *J. Clin. Invest.* **124**, 528–542 (2014).

26. M. Deng, X. Gui, J. Kim, L. Xie, W. Chen, Z. Li, L. He, Y. Chen, H. Chen, W. Luo, Z. Lu, J. Xie, H. Churchill, Y. Xu, Z. Zhou, G. Wu, C. Yu, S. John, K. Hirayasu, N. Nguyen, X. Liu, F. Huang, L. Li, H. Deng, H. Tang, A. H. Sadek, L. Zhang, T. Huang, Y. Zou, B. Chen, H. Zhu, H. Arase, N. Xia, Y. Jiang, R. Collins, M. J. You, J. Homsi, N. Unni, C. Lewis, G.-Q. Chen, Y.-X. Fu, X. C. Liao, Z. An, J. Zheng, N. Zhang, C. C. Zhang, LILRB4 signalling in leukaemia cells mediates T cell suppression and tumour infiltration. *Nature* **562**, 605–609 (2018).

27. N. Tsurutani, P. Mittal, M.C. St. Rose, S. M. Ngoi, J. Svedova, A. Menoret, F. B. Treadway, R. Laubenbacher, J. E. Suárez-Ramírez, L. S. Cauley, A. J. Adler, A. T. Vella, Costimulation endows immunotherapeutic CD8 T cells with IL-36 responsiveness during aerobic glycolysis. *J. Immunol.* **196**, 124–134 (2016).

28. F. Veglia, M. Perego, D. Gabrilovich, Myeloid-derived suppressor cells coming of age. *Nat. Immunol.* **19**, 108–119 (2018).

29. G. Germano, R. Frapolli, C. Belgiovine, A. Anselmo, S. Pesce, M. Liguori, E. Erba, S. Uboldi, M. Zucchetti, F. Pasqualini, M. Nebuloni, N. van Rooijen, R. Mortarini, L. Beltrame, S. Marchini, I. Fuso Nerini, R. Sanfilippo, P. G. Casali, S. Pilotti, C. M. Galmarini, A. Anichini, A. Mantovani, M. D'Incalci, P. Allavena, Role of macrophage targeting in the antitumor activity of trabectedin. *Cancer Cell* **23**, 249–262 (2013).

30. G. Galletti, F. Caligaris-Cappio, M. T. S. Bertilaccio, B cells and macrophages pursue a common path toward the development and progression of chronic lymphocytic leukemia. *Leukemia* **30**, 2293–2301 (2016).

31. C. D. Conrady, M. Zheng, N. A. Mandal, N. van Rooijen, D. J. J. Carr, IFN-α-driven CCL2 production recruits inflammatory monocytes to infection site in mice. *Mucosal Immunol.* **6**, 45–55 (2013).

32. B. S. Hanna, F. McClanahan, H. Yazdanparast, N. Zaborsky, V. Kalter, P. M. Rößner, A. Benner, C. Dürr, A. Egle, J. G. Gribben, P. Lichter, M. Seiffert, Depletion of CLL-associated patrolling monocytes and macrophages controls disease development and repairs immune dysfunction in vivo. *Leukemia* **30**, 570–579 (2016).

33. K. Liang, A. G. Volk, J. S. Haug, S. A. Marshall, A. R. Woodfin, E. T. Bartom, J. M. Gilmore, L. Florens, M. P. Washburn, K. D. Sullivan, J. M. Espinosa, J. Cannova, J. Zhang, E. R. Smith, J. D. Crispino, A. Shilatifard, Therapeutic targeting of MLL degradation pathways in MLL-rearranged leukemia. *Cell* **168**, 59–72.e13 (2017).

34. M. Bruchard, G. Mignot, V. Derangère, F. Chalmin, A. Chevriaux, F. Végran, W. Boireau, B. Simon, B. Ryffel, J. L. Connat, J. Kanellopoulos, F. Martin, C. Rébé, L. Apetoh, F. Ghiringhelli, Chemotherapy-triggered cathepsin B release in myeloid-derived suppressor cells activates the Nlrp3 inflammasome and promotes tumor growth. *Nat. Med.* **19**, 57–64 (2013).

35. T. Haferlach, A. Kohlmann, L. Wieczorek, G. Basso, G. T. Kronnie, M.C. Béné, J. De Vos, J. M. Hernández, W.-K. Hofmann, K. I. Mills, A. Gilkes, S. Chiaretti, S. A. Shurtleff, T. J. Kipps, L. Z. Rassenti, A. E. Yeoh, P. R. Papenhausen, W.-M. Liu, P. M. Williams, R. Foà, Clinical utility of microarray-based gene expression profiling in the diagnosis and subclassification of leukemia:

Report from the International Microarray Innovations in Leukemia Study Group. *J. Clin. Oncol.* **28**, 2529–2537 (2010).

36. A. Kohlmann, T. J. Kipps, L. Z. Rassenti, J. R. Downing, S. A. Shurtleff, K. I. Mills, A. F. Gilkes, W.-K. Hofmann, G. Basso, M. C. Dell'Orto, R. Foà, S. Chiaretti, J. De Vos, S. Rauhut, P. R. Papenhausen, J. M. Hernández, E. Lumbreras, A. E. Yeoh, E. S. Koay, R. Li, W.-M. Liu, P. M. Williams, L. Wieczorek, T. Haferlach, An international standardization programme towards the application of gene expression profiling in routine leukaemia diagnostics: The Microarray Innovations in LEukemia study prephase. *Br. J. Haematol.* **142**, 802–807 (2008).

37. G. Wang, X. Lu, P. Dey, P. Deng, C. C. Wu, S. Jiang, Z. Fang, K. Zhao, R. Konaparthi, S. Hua, J. Zhang, E. M. Li-Ning-Tapia, A. Kapoor, C.J. Wu, N. B. Patel, Z. Guo, V. Ramamoorthy, T. N. Tieu, T. Heffernan, D. Zhao, X. Shang, S. Khadka, P. Hou, B. Hu, E.J. Jin, W. Yao, X. Pan, Z. Ding, Y. Shi, L. Li, Q. Chang, P. Troncoso, C. J. Logothetis, M. J. McArthur, L. Chin, Y. A. Wang, R. A. DePinho, Targeting YAP-dependent MDSC infiltration impairs tumor progression. *Cancer Discov.* **6**, 80–95 (2016).

38. H. Gal, N. Amariglio, L. Trakhtenbrot, J. Jacob-Hirsh, O. Margalit, A. Avigdor, A. Nagler, S. Tavor, L. Ein-Dor, T. Lapidot, E. Domany, G. Rechavi, D. Givol, Gene expression profiles of AML derived stem cells; similarity to hematopoietic stem cells. *Leukemia* **20**, 2147–2154 (2006).

39. D. C. Johnson, C. Y. Taabazuing, M. C. Okondo, A. J. Chui, S. D. Rao, F. C. Brown, C. Reed, E. Peguero, E. de Stanchina, A. Kentsis, D. A. Bachovchin, DPP8/DPP9 inhibitor-induced pyroptosis for treatment of acute myeloid leukemia. *Nat. Med.* **24**, 1151–1156 (2018).

40. X. Lu, J. W. Horner, E. Paul, X. Shang, P. Troncoso, P. Deng, S. Jiang, Q. Chang, D. J. Spring, P. Sharma, J. A. Zebala, D. Y. Maeda, Y. A. Wang, R. A. DePinho, Effective combinatorial immunotherapy for castration-resistant prostate cancer. *Nature* **543**, 728–732 (2017).

41. S. M. Crusz, F. R. Balkwill, Inflammation and cancer: Advances and new agents. *Nat. Rev. Clin. Oncol.* **12**, 584–596 (2015).

42. L. Wang, B. Jia, D. F. Claxton, W. C. Ehmann, W. B. Rybka, S. Mineishi, S. Naik, M. R. Khawaja, J. Sivik, J. Han, R. J. Hohl, H. Zheng, VISTA is highly expressed on MDSCs and mediates an inhibition of T cell response in patients with AML. *Onco. Targets Ther.* **7**, e1469594 (2018).

43. A. R. Pyzer, D. Stroopinsky, H. Rajabi, A. Washington, A. Tagde, M. Coll, J. Fung, M. P. Bryant, L. Cole, K. Palmer, P. Somaiya, R. Karp Leaf, M. Nahas, A. Apel, S. Jain, M. McMasters, L. Mendez, J. Levine, R. Joyce, J. Arnason, P. P. Pandolfi, D. Kufe, J. Rosenblatt, D. Avigan, MUC1-mediated induction of myeloid-derived suppressor cells in patients with acute myeloid leukemia. *Blood* **129**, 1791–1801 (2017).

44. S. Trabanelli, M. F. Chevalier, A. Martinez-Usatorre, A. Gomez-Cadena, B. Salomé, M. Lecciso, V. Salvestrini, G. Verdeil, J. Racle, C. Papayannidis, H. Morita, I. Pizzitola, C. Grandclément, P. Bohner, E. Bruni, M. Girotra, R. Pallavi, P. Falvo, E. O. Leibundgut, G. M. Baerlocher, C. Carlo-Stella, D. Taurino, A. Santoro, O. Spinelli, A. Rambaldi, E. Giarin, G. Basso, C. Tresoldi, F. Ciceri, D. Gfeller, C. A. Akdis, L. Mazzarella, S. Minucci, P. G. Pelicci, E. Marcenaro, A. N. J. McKenzie, D. Vanhecke, G. Coukos, D. Mavilio, A. Curti, L. Derré, C. Jandus, Tumour-derived PGD2 and NKp30-B7H6 engagement drives an immunosuppressive ILC2-MDSC axis. *Nat. Commun.* **8**, 593 (2017).

45. S.-H. Yu, K.-Y. Zhu, J. Chen, X.-Z. Liu, P.-F. Xu, W. Zhang, L. Yan, H.-Z. Guo, J. Zhu, JMJD3 facilitates C/EBPβ-centered transcriptional program to exert oncorepressor activity in AML. *Nat. Commun.* **9**, 3369 (2018).

46. F. O. Bagger, N. Rapin, K. Theilgaard-Mönch, B. Kaczkowski, J. Jendholm, O. Winther, B. Porse, HemaExplorer: A Web server for easy and fast visualization of gene expression in normal and malignant hematopoiesis. *Blood* **119**, 6394–6395 (2012).

47. F. O. Bagger, N. Rapin, K. Theilgaard-Mönch, B. Kaczkowski, L. A. Thoren, J. Jendholm, O. Winther, B. T. Porse, HemaExplorer: A database of mRNA expression profiles in normal and malignant haematopoiesis. *Nucleic Acids Res.* **41**, D1034–D1039 (2013).

48. S. Heinz, C. E. Romanoski, C. Benner, K. A. Allison, M. U. Kaikkonen, L. D. Orozco, C. K. Glass, Effect of natural genetic variation on enhancer selection and function. *Nature* **503**, 487–492 (2013).

49. N. T. Hogan, M. B. Whalen, L. K. Stolze, N. K. Hadeli, M. T. Lam, J. R. Springstead, C. K. Glass, C. E. Romanoski, Transcriptional networks specifying homeostatic and inflammatory programs of gene expression in human aortic endothelial cells. *eLife* **6**, e22536 (2017).

50. S. Mei, Q. Qin, Q. Wu, H. Sun, R. Zheng, C. Zang, M. Zhu, J. Wu, X. Shi, L. Taing, T. Liu, M. Brown, C. A. Meyer, X. S. Liu, Cistrome Data Browser: A data portal for ChIP-Seq and chromatin accessibility data in human and mouse. *Nucleic Acids Res.* **45**, D658–D662 (2017).